

## Correlations between intratumoral interstitial fibrillary network and tumoral architecture in prostatic adenocarcinoma

A. STOICULESCU<sup>1,2)</sup>, I. E. PLEŞEA<sup>2)</sup>, O. T. POP<sup>3)</sup>, D. O. ALEXANDRU<sup>4)</sup>,  
 M. MAN<sup>5)</sup>, M. ŞERBĂNESCU<sup>2)</sup>, R. M. PLEŞEA<sup>2)</sup>

<sup>1)</sup>Department of Urology,  
 Emergency County Hospital, Pitesti

<sup>2)</sup>Department of Pathology

<sup>3)</sup>Research Center for Microscopic Morphology and Immunology

<sup>4)</sup>Department of Medical Informatics  
 University of Medicine and Pharmacy of Craiova

<sup>5)</sup>Department of Pathology,  
 Emergency County Hospital, Pitesti

### Abstract

The authors made a preliminary assessment of possible correlations between the amount of intratumoral stromal fibrillary components (ISFC) and the architectural tumoral patterns described by Gleason. The studied material consisted of samples obtained by transurethral resection from 34 patients diagnosed with prostatic adenocarcinoma. Ten fields, five for dominant and five for secondary identified patterns of each case, with no necrosis were selected randomly from Gömöri stained sections using ×20 objective. ISFC-ratio increased with Gleason pattern both for the entire group but also for “Necrotizing” phenotype patterns and “Solid” phenotype patterns, excepting the subtype “4A” where the stromal compartment was reduced by the expansion of tumoral ducts enlarged by growing tumoral intraductal cribriform masses. These preliminary data showed that stromal microenvironment try to adapt to the loss of tumoral differentiation by increasing the amount of fibrillary components of intratumoral stromal compartment.

**Keywords:** prostate carcinoma, Gleason pattern, stroma.

### Introduction

Currently, prostate carcinoma (PC) is, according to the latest official statistics of *WHO*, including data up to 2008, the second most common malignancy when it comes to occurrence and diagnosis in men, surpassed only by lung cancer, and the fifth most common malignancy in general, surpassed by lung, breast, colorectal and gastric cancer. Also, since 2011, PC is the sixth leading cause of cancer death in men worldwide [1, 2]. However, both in Europe and in the USA, the last official statistics of *WHO* in 2008 placed the PC first, before the lung, in terms of the number of new cases. The same statistics show that, in terms of mortality, PC is placed in 2008 on the third position in Europe after lung and colorectal cancer, and the second position in the U.S., after lung cancer [3, 4].

In the last three quarters of the twentieth century, more than 40 systems establishing the degree of differentiation (DD) and staging of prostate cancer were proposed, pathologists worldwide oscillating in adopting one system or another [5]. The classification system most widely used worldwide, both in research and current medical practice, is designed and developed by Dr. Donald F. Gleason, pathologist from Minnesota, and members of the “Veterans Administration Cooperative Urological Research Group” (VACURG) [6–12].

Evaluation and classification algorithm is based on two fundamental criteria: the degree of glandular differentiation and tumor development pattern in prostatic stroma [10].

Prostatic stroma is a complex structure, which, like any other stroma, consists of two main components: specific cellular component and the extracellular matrix, which, in turn, includes a structured fibrillary component and an unstructured, amorphous component, *i.e.* ground substance [13–15]. The main types of stromal cells in prostate are: the smooth muscle cells, the fibroblasts and the myofibroblasts, the former, representing the most numerous contingent [16, 17].

In 1992, Cunha GR *et al.* demonstrated that mesenchymal–epithelial interactions play a key role in the development of the male urogenital tract in that the mesenchyme causes and states the patterns of epithelial morphogenesis, regulates epithelial proliferation, triggers epithelial cytodifferentiation and causes as well as specifies the functional or biochemical activity of the epithelium [18]. Further studies demonstrated that these stromal–epithelial interactions change also the proliferation, the adhesion and the motility of malignant cells, thus influencing the evolution and progression of PC [19].

Since 1998, a new concept was introduced and

developed, *i.e.* “reactive stroma”, to define the intra-tumoral stroma of PC which was proved to be different from stroma of the normal prostate [20, 21] and to be responsible for the genesis and development of PC and for promoting its invasion, progression and metastasis [22]. De Wever O and Mareel M unified, in 2003, all previous observations concerning the relationship between tumoral stroma and malignant cells, describing two main pathways of the stromal–epithelial interactions: the afferent pathway in which reactive stroma directs the carcinogenesis of prostate epithelia and cancer progression and efferent pathway in which stromal cells are activated by cancer tissue [23].

The literature of the last decade contains an overwhelming number of studies dedicated to prostate tumor stroma and its interactions with the population of malignant cells but only very few of them address the quantitative relationship between different components of the tumor stroma and tumor parenchyma. Based on these considerations, the present study aims at analyzing the relationship between the amount of fibrillar material within the tumor microenvironment and the degree of differentiation of tumor parenchyma in prostate carcinoma assessed using the Gleason system.

## Materials and Methods

The basis for this study was represented by a group of 34 patients admitted with suspected nodular benign prostatic hyperplasia (NBH) who underwent transurethral resection (TURP), in whom the postoperative histopathological examination established the presence of malignant carcinomatous proliferation invading the NBH area. Thus, the discovery of the carcinoma was incidental and the patients underwent no specific previous treatment.

Prostate tissue fragments were collected by TURP, fixed in 10% buffered formalin and embedded in paraffin. Serial sections were cut from the paraffin blocks and were stained in each case according to the algorithm shown in Table 1.

**Table 1 – Staining procedures used in the study**

Section	Stain	Goal
S 1	HE	Setting of Gleason patterns
S 2	Trichrome van Gieson	Qualitative assessment of intratumoral stroma
S 3	Trichrome Goldner	
S 4	SMA (IHC)	
S 5	Gömöri technique	Qualitative assessment of stromal fibrillary compound

For the immunohistochemical staining, sections were placed on SuperFrost+ slides and three-stage indirect Streptavidin–Biotin Complex (SaBC)/Horseradish peroxidase (HRP) method was used. For visualization, we used the DAB chromogen and Hematoxylin counterstaining. Anti-Smooth Muscle Actin antibody was used, clone 1A4 (DAKO), with a dilution of 1:50.

The parameters taken into consideration to be studied were:

- the architectural development pattern of prostate carcinoma assessed using the Gleason system;
- the percentage of the intratumoral stromal fibrillary component (ISFC).

In each of the 34 cases, we assessed the two main architectural patterns: the dominant pattern and the secondary pattern. For each pattern, five randomly selected fields without necrosis at  $\times 20$  magnification were selected. Thus, in each case we selected 10 tumor areas. The final batch was thus composed of 340 tumor areas. The 340 tumor tissue samples were assigned to the five main groups of tumor architectural aspects described by Gleason and their variants.

Two additional groups were designed, according to Gleason diagram of pattern subtypes:

- the “necrotizing phenotype” group, including the subtypes 3C, 4A and 5A, in which tumoral proliferation seems to evolve towards solid individual masses with central necrosis, passing through a cribriform stage;
- the “solid phenotype” group, including the subtypes 3A, 3B, 4B and 5B in which tumoral proliferation seems to evolve from well differentiated glandular aspects of pattern 2 towards solid variable clusters of undifferentiated tumoral cells of 5B subtype.

ISFC quantitative morphometric measurements were performed using the “Measurements” module of the Analysis Pro 5.0 software.

For assessing the ISFC percentage, we used the “S5” sections stained using the Gömöri silver impregnation technique, which identifies all collagen fibers, including reticular ones, generally considered to be newly formed and unorganized young collagen fibers.

Values were grouped into four classes for the stromal component density score, shown in Table 2.

**Table 2 – Scale of ISFC ratio values**

Score	Ratio values
D 1	<10%
D 2	10–20%
D 3	20–30%
D 4	>30%

For each pattern, we assessed: the lowest value (VMIN); the highest value (VMAX); the half range value (HRV); mean value (AV); standard deviation (STDEV).

For comparison between stromal component percentage mean values of different Gleason patterns and subtypes the Student *t*-test was used. For comparison between stromal component percentage values distributions of different Gleason patterns and subtypes, the Kolmogorov–Smirnov test (K-S test) was used. For comparison of stromal component percentage values in different Gleason patterns divided into score classes according to the scale presented above, the  $\chi^2$ -test was used.

## Results

The most numerous were the moderately and poorly differentiated patterns (3, 4 and 5) (Figure 1).

### General assessment

The amount of IFSC varied within wide ranges of values, whose lowest limit (2.77%) was observed in the pattern 5 group of samples, and highest limit in the pattern 3 group of samples (61.59%) The largest range was observed in the pattern 5 group of samples (Table 3, Figures 2 and 3).

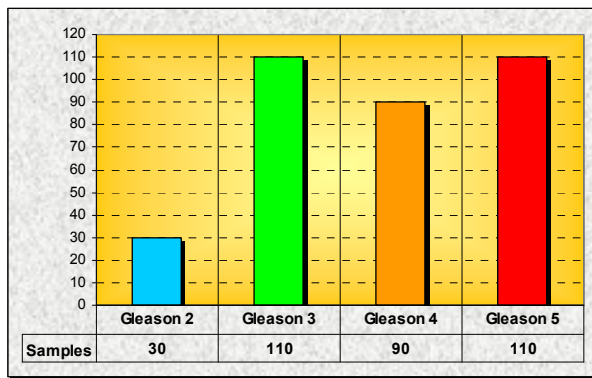


Figure 1 – Distribution of determinations according to Gleason patterns.

Table 3 – Distribution of main statistical parameters in Gleason patterns

Parameter	Value			
	GL 2	GL 3	GL 4	GL 5
No. of samples	30	110	90	110
VMIN	9.7	8.35	6.65	2.77
VMAX	46.42	61.59	50.76	59.57
HRV	28.08	34.97	28.71	31.17
AV	21.44	24.57	21.81	33.07
STDEV	9.36	9.22	9.99	11.76
AV + STDEV	30.8	33.78	31.80	44.83
AV - STDEV	12.1	15.35	11.82	21.31

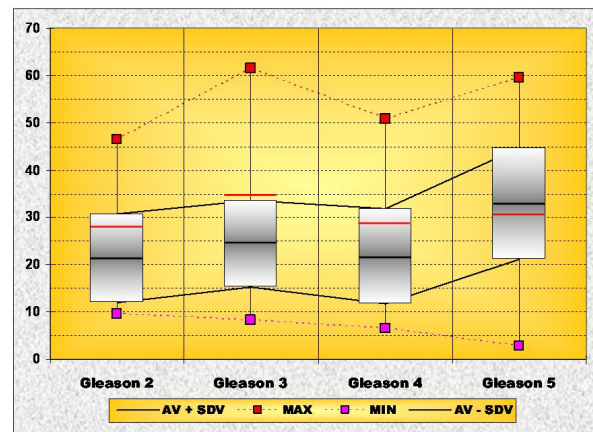


Figure 2 – Comparative representation of main statistical parameters of Gleason patterns.

However, in spite of this dispersion, in all pattern groups, most values were “aggregated” in ranges of smaller and almost similar amplitudes, determined by relatively close STDEV values around the AV values of each group (Table 3, Figure 2).

Excepting the Gleason 5 group, in all the other pattern groups the AV amount of ISFC had a smaller value than the HRV, the intervals including the majority of values being thus displaced on the lower limit of the ranges (Table 3, Figure 2).

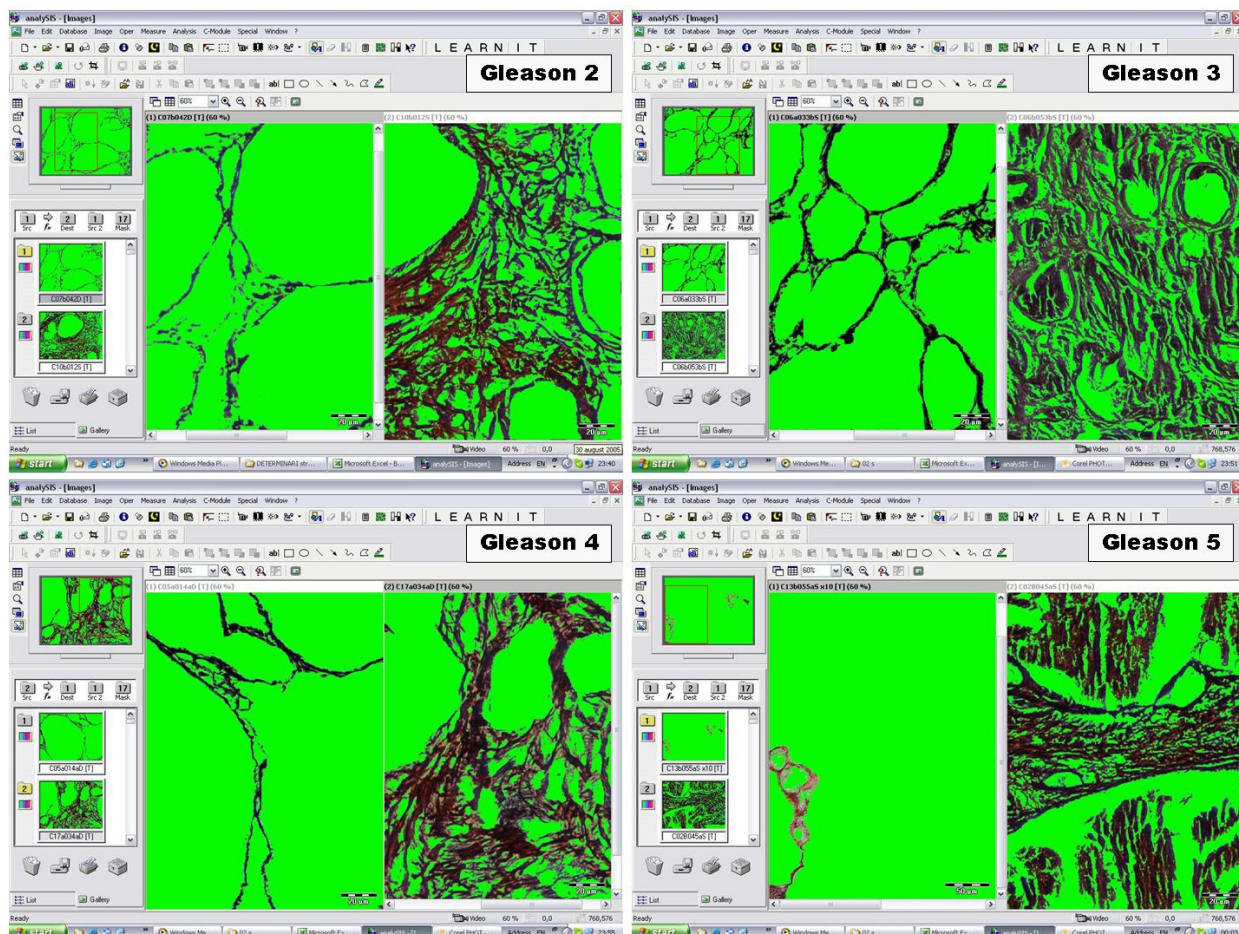


Figure 3 – The windows of image analysis program showing the ISFC lowest and highest values in Gleason groups.

The most interesting observation was that AV values had an ascending trend from pattern 2 to pattern 5,

excepting pattern 4 whose AV was similar to pattern 2 value (Table 3, Figure 2).

The statistical comparison between ISFC mean values of Gleason main groups using Student *t*-test, confirmed the close similarity between the AVs of Gleason 2 and Gleason 4 groups but also a similarity between Gleason 2 and Gleason 3 groups, for the rest of comparisons, Student test underlining the differences between the AVs (Figure 2, Table 4).

**Table 4 – Statistical comparison between ISFC mean values in Gleason patterns**

Student <i>t</i> -test	Gleason 2	Gleason 3	Gleason 4
Gleason 2			
Gleason 3	0.103 (>0.05)		
Gleason 4	0.857 (>0.05)	<b>0.044 (&lt;0.05)</b>	
Gleason 5	<b>&lt;0.0001</b>	<b>&lt;0.0001</b>	<b>&lt;0.0001</b>

The analysis of the main statistical parameters in the subtypes of Gleason patterns from 3 to 5 revealed some

interesting aspects. A wide dispersion of values was noticed in at least one subtype as compared to the other subtypes of the main patterns, *i.e.* 4B in group 4, 3B in group 3 and especially 5A in group 5. The intervals comprising the majority of values (as defined by the STDEVs around AVs) were generally more “condensed” than the corresponding ranges and were almost similar, excepting Gleason 5A subtype which had the widest limits, more than twice as large as the others. In pattern 3 subtypes, these intervals had almost the same wideness. They were more homogenously placed in subgroups 3A and 3C, near the middle of the corresponding ranges whereas in subgroup 3B the interval was obviously displaced on the lower limit of the range, due to the smaller AV value as compared to the corresponding HRV value. However, the AV values had an ascending trend from 3A subgroup to 3C subgroup (Figure 4).

Parameter	Value						
	GL 3A	GL 3B	GL 3C	GL 4A	GL 4B	GL 5A	GL 5B
No. Samples	50	40	20	70	20	30	80
VMIN	8.35	11.40	13.14	6.65	7.97	2.77	12.98
VMAX	36.96	61.59	43.23	40.94	50.76	59.57	48.63
HRV	22.65	36.5	28.18	23.8	29.36	31.17	30.8
AV	<b>21.57</b>	<b>27.00</b>	<b>27.19</b>	<b>20.06</b>	<b>27.94</b>	<b>32.27</b>	<b>33.37</b>
STDEV	<b>8.59</b>	<b>9.73</b>	<b>7.7</b>	<b>8.48</b>	<b>12.46</b>	<b>18.87</b>	<b>7.73</b>
AV + STDEV	30.17	36.73	34.89	28.54	40.40	51.14	41.11
AV - STDEV	12.98	17.26	19.49	11.58	15.48	13.41	25.64

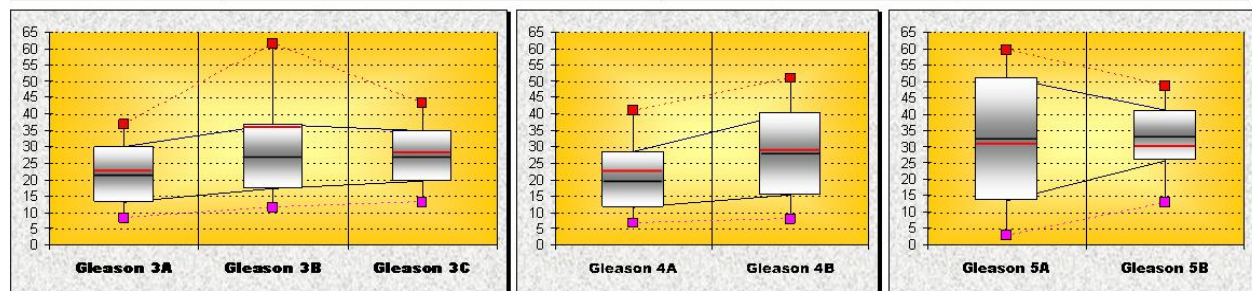


**Figure 4 – Distribution and comparative representation of main statistical parameters in Gleason subgroups.**

The statistical comparison between ISFC mean values of Gleason 3 subtypes using Student *t*-test, confirmed, on one hand, the differences between the AVs of 3A and 3B subtypes and 3A and 3C subtypes and, on the other hand, underlined the similarity between the AVs of 3B and 3C subtypes (Table 5).

**Table 5 – Statistical comparison between ISFC mean values in Gleason pattern subtypes**

Student <i>t</i> -test	Gleason 3A	Gleason 3B	Gleason 4B	Gleason 5B
Gleason 3A				
Gleason 3B	<b>0.006 (&lt;0.05)</b>			
Gleason 3C	<b>0.013 (&lt;0.05)</b>	0.937 (>0.05)		
Gleason 4A			<b>0.001 (&lt;0.05)</b>	
Gleason 5A				0.664 (>0.05)

In pattern 4, the amount of IFSC expressed different distributions in the two subtypes. Thus, in subtype 4a the whole range of values was smaller, the interval

comprising the majority of values was more “condensed” around an AV value smaller than the HRV, which displaced the interval on the lower limit of the range, whereas in subtype 4B both the whole range and the interval comprising the majority of values were larger and the AV value, higher than that of the other subgroup, but almost equal to the HRV placed the interval comprising the majority of values in the middle of the whole range. The statistical comparison of the AVs of Gleason 4 subtypes using Student *t*-test, confirmed the evident difference between them (Table 5).

In pattern 5, the amount of ISFC also had different models of distribution in the two subtypes. Whereas in subtype 5A both the whole range and the interval comprising the majority of values were very large (the largest in the entire group of determinations), in subtype 5B both ranging intervals were narrow. However, the AV value was only slightly higher in the 5B subtype than in the 5A subtype, fact confirmed also by the statistical comparison using Student *t*-test (Table 5) but both were higher than the corresponding HRVs. Finally,

if we follow the AVs from subgroup 3A to subgroup 5B we can clearly observe that they are “articulated” in a smooth ascending scale which has a “broken” step only in the 4A subtype, where the AV value of the ISFC amount is smaller than that of the 3A subtype (Figure 4) and even than that of pattern 2 (Table 3, Figure 2).

### “Necrotizing” phenotype

In the “necrotizing” phenotype group there are two aspects revealed by the analysis of the main statistical parameters. The first one is the discrepancy between the whole ranges and intervals comprising the majority of values in subtypes 3C and 4A on one hand, and the corresponding intervals in subtype 5A on the other hand. Whereas in the former subtypes both intervals are more “condensed”, in the latter both intervals are “expanded” (Table 6, Figures 5 and 6).

**Table 6 – Distribution of main statistical parameters in subtypes of “Necrotizing” phenotype**

Parameter	Value		
	GL 3c	GL 4a	GL 5a
No. of samples	20	70	30
VMIN	13.14	6.65	2.77
VMAX	43.23	40.94	59.57
HRV	28.18	23.8	31.17
AV	<b>27.19</b>	<b>20.06</b>	<b>32.27</b>
STDEV	<b>7.7</b>	<b>8.48</b>	<b>18.87</b>
AV + STDEV	34.89	28.54	51.14
AV - STDEV	19.49	11.58	13.41

The second important aspect is that AV values seem to have a slightly ascending trend from subgroup 3C to subgroup 5A but with an obvious “gap” in subgroup 4A (Table 6, Figure 6).

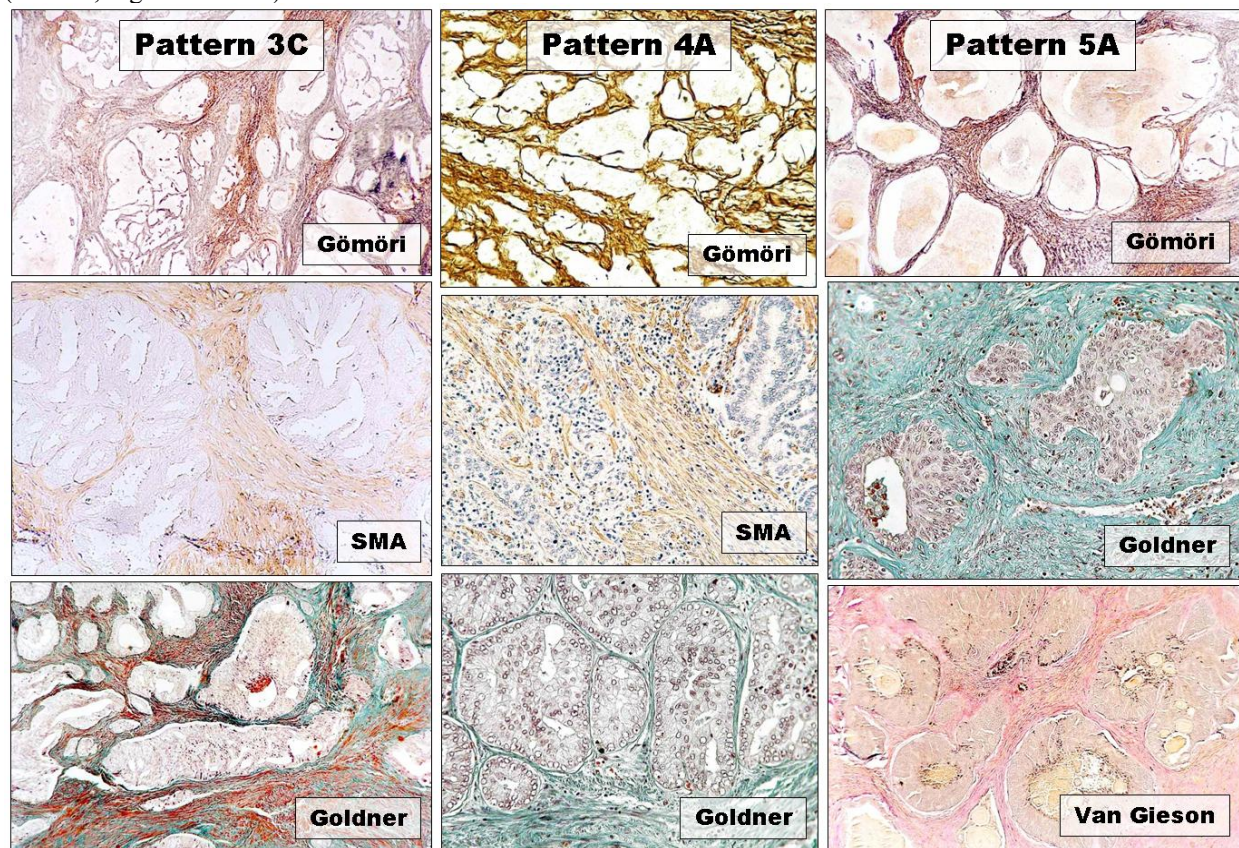


**Figure 5 – Different aspects of tumoral stroma in “Necrotizing” phenotype subtypes of Gleason patterns.**

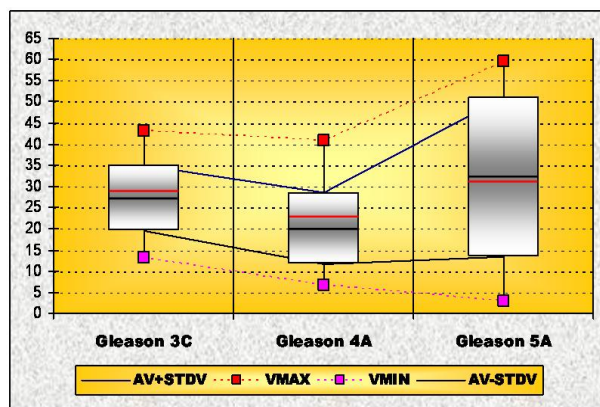


**Figure 6 – Comparative representation of the main statistical parameters in subtypes of “Necrotizing” phenotype.**

However, the difference between AVs of 3C and 5A subtypes is not statistically validated by Student *t*-test, whose *p*-value is higher than the significance level of 0.05 (Table 7).

**Table 7 – Statistical comparison between ISFC mean values in subtypes of “Necrotizing” phenotype**

Student <i>t</i> -test	Gleason 3C	Gleason 4A
Gleason 3C		
Gleason 4A	<b>0.001 (&lt;0.05)</b>	
Gleason 5A	0.260 (>0.05)	<b>&lt;0.0001</b>

### “Solid” phenotype

In the “solid” phenotype subtypes, the situation is different from the one described above. Although the whole ranges are significantly variable, with the largest wideness in the 3B subgroup, the intervals comprising the

majority of values are more homogenously “condensed” around AVs that are continuously and smoothly increasing from subgroup 3A to subgroup 5B (Table 8, Figures 7 and 8).

**Table 8 – Distribution of main statistical parameters in subtypes of “Solid” phenotype**

Parameter	Value			
	GL 3a	GL 3b	GL 4b	GL 5b
No. of samples	50	40	20	80
VMIN	8.35	11.40	7.97	12.98
VMAX	36.96	61.59	50.76	48.63
HRV	22.65	36.5	29.36	30.8
AV	<b>21.57</b>	<b>27.00</b>	<b>27.94</b>	<b>33.37</b>
STDEV	8.59	9.73	12.46	7.73
AV + STDEV	30.17	36.73	40.40	41.11
AV - STDEV	12.98	17.26	15.48	25.64

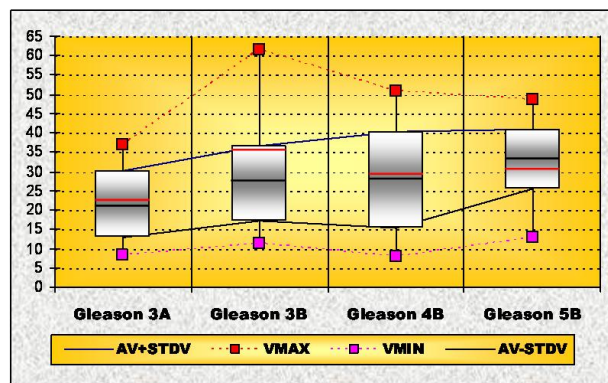


**Figure 7 – Comparative representation of main statistical parameters in subtypes of “Solid” phenotype.**

However, in 4B subtype, the interval comprising the majority of values around AV was more extended than in the other subtypes of “Solid” phenotype.

The AV amount of ISFC had a smaller value than the HRV, starting from 3A subtype to 4B subtype, the intervals including the majority of values being thus displaced towards the lower limit of the ranges. In contrast, in 5B subtype, the AV was higher than the HRV, thus displacing the interval including the majority of values on the upper limit of the range (Table 8, Figure 7).

The statistical comparison between ISFC mean values of “Solid” phenotype subtypes using Student test, confirmed the close similarity between the AVs of 3B and 4B subtypes (Table 9, Figure 7).

**Table 9 – Statistical comparison between ISFC mean values in subtypes of “Solid” phenotype**

Student <i>t</i> -test	GL 3a	GL 3b	GL 4b
GL 3a			
GL 3b	<b>0.006</b> ( $<0.05$ )		
GL 4b	<b>0.017</b> ( $<0.05$ )	0.748 ( $>0.05$ )	
GL 5b	<b>&lt;0.0001</b>	<b>0.0001</b> ( $<0.05$ )	<b>0.016</b> ( $<0.05$ )

For the rest of comparisons, Student *t*-test underlined the differences between the AVs, sustaining thus the idea of an ascending trend of AV amount of ISFC in “Solid” phenotype from better to poorly differentiated tumoral areas.

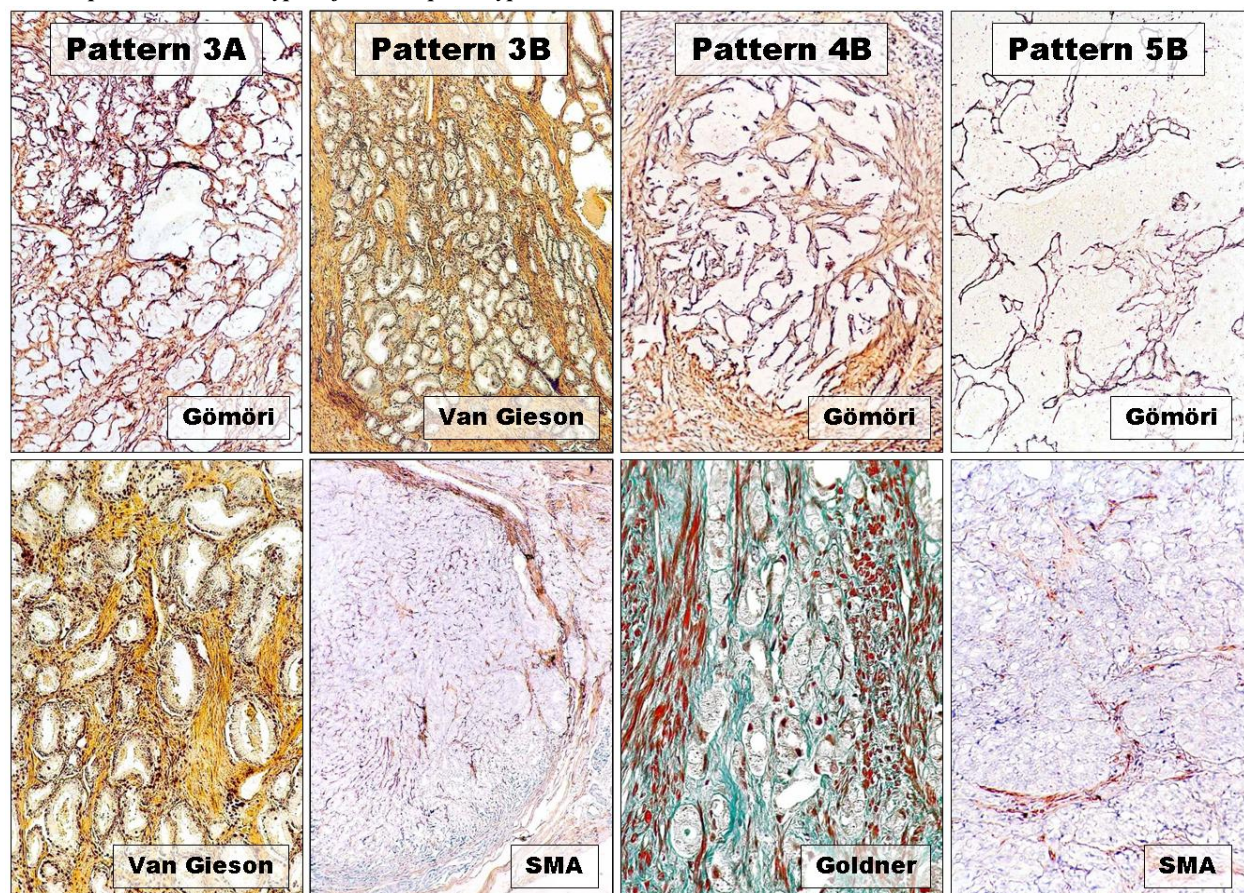


**Figure 8 – Different aspects of tumoral stroma in “Solid” phenotype subtypes of Gleason patterns.**

## Discussion

Since 1996, Cunha GR *et al.* stated that as the prostatic tumor grade is increasing the amount of stroma smooth muscle is decreasing by dedifferentiation [16]. Further studies detailed that, in the reactive stroma, this evident morphologic event, consisting of a progressive significant decrease or loss of smooth muscle cells is concomitant with a myofibroblasts and fibroblasts proliferation and a corresponding amplification of the corresponding extracellular matrix compounds [17, 23, 24].

### General assessment

The amount of ISFC had an overall increasing trend from well-differentiated patterns towards poorly differentiated ones. Thus, while in half of pattern 2 areas ISFC occupied between 10% and 20% of tumoral area, in almost two third of pattern 5 areas the amount of ISFC was higher than 30% of tumoral area (Table 10, Figure 9).

**Table 10 – “P” values of K–S test comparison between distributions of ISFC values in Gleason patterns**

K–S test	Gleason 2	Gleason 3	Gleason 4
Gleason 2			
Gleason 3	0.053 (>0.05)		
Gleason 4	0.45 (>0.05)	0.004 (<0.05)	
Gleason 5	<0.0001	<0.0001	<0.0001

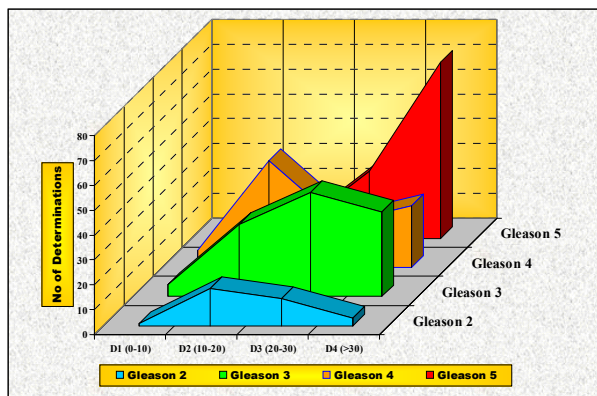


**Figure 9 – Graphic representation of different ISFC ratio values distributions in Gleason patterns.**

This trend is “disturbed” between pattern 3 and

pattern 5 by the distribution of ISFC ratio classes of pattern 4, which is almost similar to that of pattern 2, with a predominance of tumoral areas having an ISFC amount smaller than 20%, similarity confirmed also by the used statistical tools (Table 11, Figure 10).

**Table 11 – “P” values of  $\chi^2$ -test comparison between distributions of ISFC classes in Gleason patterns**

$\chi^2$ -test	GL 2	GL 3	GL 4	General
GL 2				
GL 3	0.042			
GL 4	0.094	0.005		
GL 5	<0.0001	<0.0001	<0.0001	
General				<0.0001

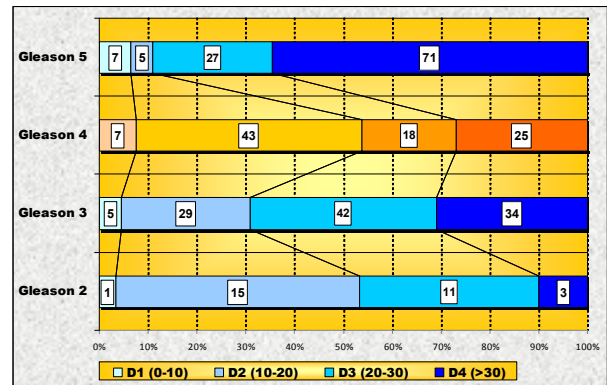


**Figure 10 – Graphic representation of different ISFC ratio classes’ proportions in Gleason patterns.**

The analysis of the ISFC amount trend within each Gleason pattern revealed differences, sometimes important, between the subtypes. Thus, in Gleason 3 pattern, there is a slightly increasing trend of ISFC amount from subtype 3A towards subtype 3C, very smooth however from subtype 3B towards type 3C (Tables 12 and 13, Figures 11 and 12).

In Gleason pattern 4, in turn, the difference between the two subtypes is striking. Thus, while in subtype 4B the amount of ISFC follows the general rule, with a predominance of tumoral areas having more than 30% of their surface occupied by ISFC, in Gleason 4A subtype the situation is totally opposite, almost two thirds of tumoral areas having an amount of ISFC smaller than 20% of their surface (Tables 12 and 13, Figures 11 and 12).

K-S Test	Gleason 3a	Gleason 3b	Gleason 4b	Gleason 5b
Gleason 3a				
Gleason 3b	0,0502 (>0,05)			
Gleason 3c	0,031 (<0,05)	0,644 (>0,05)		
Gleason 4a			0,025 (<0,05)	
Gleason 5a				0,028 (<0,05)

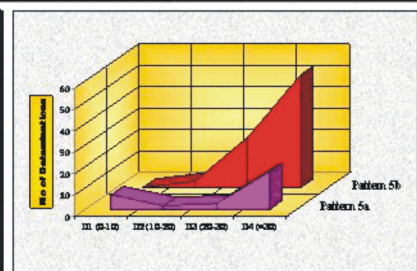
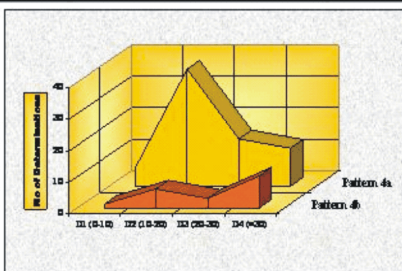
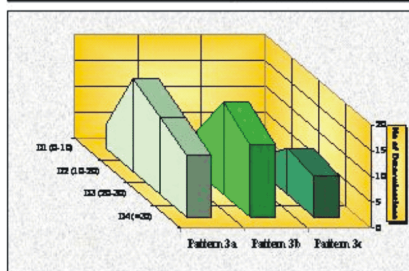


**Table 12, Figure 11 – “P” values of K–S test comparison between distributions of ISFC values in Gleason subtypes and graphic representation of these distributions.**

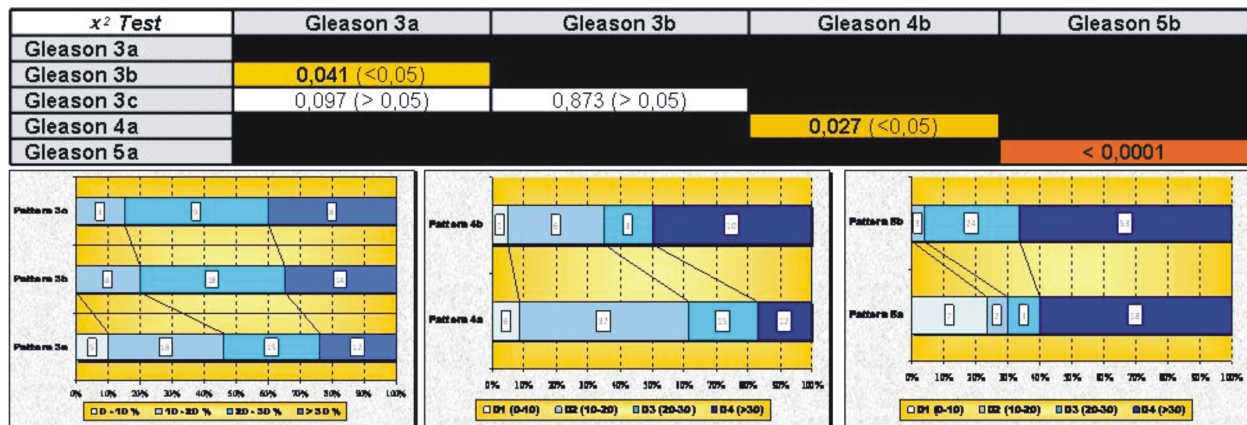


Table 13, Figure 12 – “P” values of  $\chi^2$ -test comparison between distributions of ISFC ratio classes in Gleason subtypes and graphic representation of these proportions.

In Gleason pattern 5, the situation is comparable with that observed in pattern 3 group but with a particular aspect: while in 5B subtype almost all determined values of ISFC amount were higher than 20% and especially higher than 30%, in 5A subtype a significant proportion of determined values, *i.e.* almost one fourth, were smaller than 10% (Tables 12 and 13, Figures 11 and 12).

### “Necrotizing” phenotype

The overall trend of ISFC amount in “Necrotizing” subtypes was to increase from well-differentiated type 3C towards poorly differentiated type 5A. The 4A well-defined cribriform areas went obviously out of the pattern described, showing predominantly a “contraction” of stromal spaces (Tables 14 and 15, Figures 13 and 14), which became almost like or more narrow than those of Gleason 2 pattern (Figure 4). These observations could support the idea of a distinct phenotype of malignant cells, with an accelerated pattern of proliferation within the tumoral glands, resulting in their rapid enlargement with a consecutive narrowing of the interstitial spaces rather than their invasion. In the next step, central necrosis appears in these large tumoral masses, resulting in their “contraction” with a consecutive re-expansion of the stromal microenvironment.

Table 14 – “P” values of K-S test comparison between distributions of ISFC values in “Necrotizing” phenotype group of patterns

K-S test	Gleason 3c	Gleason 4a
Gleason 3c		
Gleason 4a	0.002 (<0.05)	
Gleason 5a	0.024 (<0.05)	<0.0001

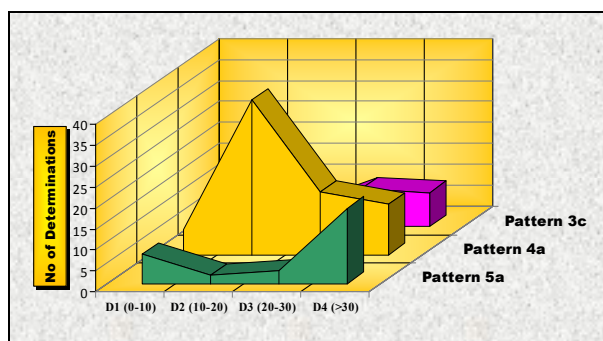


Figure 13 – Graphic representation of different ISFC ratio values distributions in “Necrotizing” phenotype.

Table 15 – “P” values of  $\chi^2$ -test comparison between distributions of ISFC classes in “Necrotizing” phenotype group of patterns

$\chi^2$ -test	GL 3c	GL 4a	General
GL 3c			
GL 4a	0.003		
GL 5a	0.006	<0.0001	
General			<0.0001

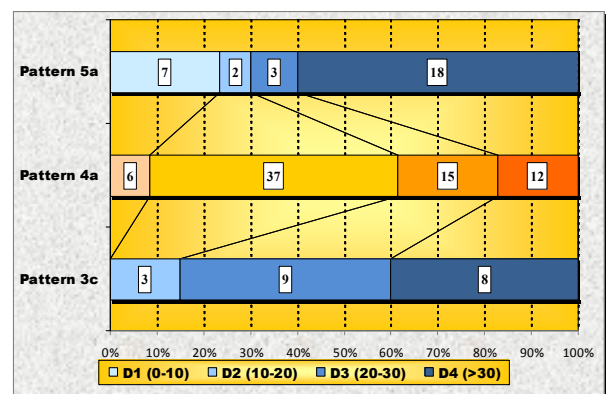


Figure 14 – Graphic representation of different ISFC ratio classes’ proportions in “Necrotizing” phenotype group of patterns.

### “Solid” phenotype

In what we called as “Solid” phenotype group of Gleason subtypes the increasing trend of ISFC amount from well-differentiated subtypes towards the poorly differentiated ones was more obviously continuous, with no “artifacts” like in “Necrotizing” group (Tables 16 and 17, Figures 15 and 16).

However, the 4B subtype showed a rather significant number of areas – one fourth – with narrowed interstitial spaces but in two thirds of areas ISFC amount was larger than 20% and especially larger than 30%.

Table 16 – “P” values of K-S test comparison between distributions of ISFC values in “Solid phenotype” group of patterns

K-S test	GL 3a	GL 3b	GL 4b
GL 3a			
GL 3b	0.0502 (>0.05)		
GL 4b	0.089 (>0.05)	0.358 (>0.05)	
GL 5b	<0.0001	0.0001 (<0.05)	0.033 (<0.05)

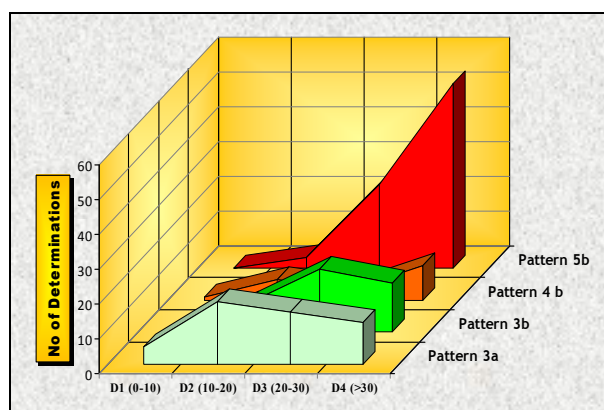


Figure 15 – Graphic representation of different ISFC ratio values distributions in “Solid” phenotype.

Table 17 – “P” values of  $\chi^2$ -test comparison between distributions of ISFC classes in “Solid” phenotype group of patterns

$\chi^2$ -test	GL 3a	GL 3b	GL 4b	General
GL 3a				
GL 3b	0.041			
GL 4b	0.180	0.080		
GL 5b	<0.0001	0.001	<0.0001	
	General			<0.0001

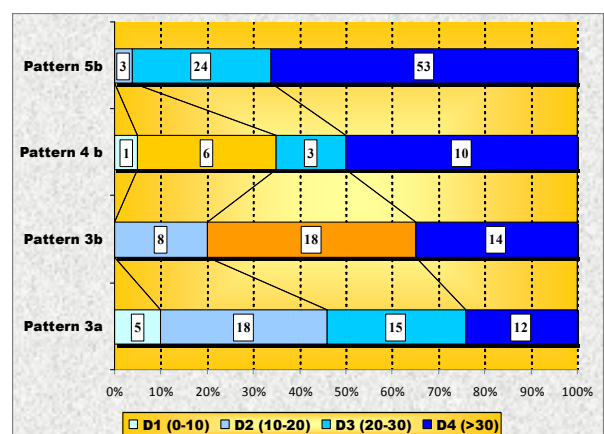


Figure 16 – Graphic representation of different ISFC ratio classes’ proportions in “Solid” phenotype group of patterns.

## Conclusions

The tumoral stromal environment showed, through its fibrillary component, a tendency to expansion parallel to that of the reduction of the tumor differentiation degree expressed by the Gleason patterns. However, the noted upward trend of the fibrillary component percentage recorded an “artifact” in pattern “4” obviously caused by the situation encountered in its predominant “4A” subtype in which the stromal environment was reduced, probably due to the “distension” of the glandular channels triggered by an important and compact intracanalicular cribriform tumor mass with rapid growth. This subtype clearly made the difference also between the ISFC amount trend in the two-defined groups – “Necrotizing” and “Solid” – suggesting the existence of two phenotypically different malignant cell populations

interacting distinctly with intratumoral microenvironment.

## Acknowledgments

This study represents part of the final results of two research projects: No. 255/2003 and No. 445/2004, supported by grant from the Ministry of Education and Research through “VIASAN” PROGRAM.

## References

- [1] Jemal A, Bray F, Center MM, Ferlay J, Ward E, Forman D, *Global cancer statistics*, CA Cancer J Clin, 2011, 61(2):69–90.
- [2] IARC (International Agency for Research on Cancer), *GLOBOCAN 2008 database (version 1.2)*, <http://globocan.iarc.fr>, 2008.
- [3] American Cancer Society, *Cancer Facts and Figures 2010*, [http://www.cancer.org/acs/groups/content/@epidemiology\\_surveillance/documents/document/acspc-026238.pdf](http://www.cancer.org/acs/groups/content/@epidemiology_surveillance/documents/document/acspc-026238.pdf), Accessed January 19, 2011.
- [4] Ferlay J, Parkin DM, Steliarova-Foucher E, *Estimates of cancer incidence and mortality in Europe in 2008*, Eur J Cancer, 2010, 46(4):765–781.
- [5] Humphrey PA, Grading of prostatic carcinoma (Chapter 15). In: \*\*, *Prostate pathology*, ASCP Press, Chicago, 2003, 338–374.
- [6] Gleason DF, *Classification of prostatic carcinoma*, Cancer Chemother Rep, 1966, 50(3):125–128.
- [7] Mellinger GT, Gleason D, Bailar J 3<sup>rd</sup>, *The histology and prognosis of prostatic cancer*, J Urol, 1967, 97(2):331–337.
- [8] Gleason DF, Mellinger GT, *Prediction of prognosis for prostatic adenocarcinoma by combined histological grading and clinical staging*, J Urol, 1974, 111(1):58–64.
- [9] Gleason DF, The Veterans Administration Cooperative Urological Research Group. Histologic grading and clinical staging of prostatic carcinoma. In: Tannenbaum M (ed), *Urologic pathology: the Prostate (Chapter 9)*, Lea & Febiger, Philadelphia, 1977, 171–197.
- [10] Gleason DF, Histologic grading of prostatic carcinoma. In: Bostwick DG (ed), *Pathology of the prostate*, Churchill Livingstone, New York, 1990, 83–93.
- [11] Gleason DF, *Histologic grading of prostate cancer: a perspective*, Hum Pathol, 1992, 23(3):273–279.
- [12] Humphrey PA, *Gleason grading and prognostic factors in carcinoma of the prostate*, Mod Pathol, 2004, 17(3):292–306.
- [13] Aumüller G, *Morphologic and endocrine aspects of prostatic function*, Prostate, 1983, 4(2):195–214.
- [14] Hayward SW, *Approaches to modeling stromal-epithelial interactions*, J Urol, 2002, 168(3):1165–1172.
- [15] Laczkó I, Hudson DL, Freeman A, Feneley MR, Masters JR, *Comparison of the zones of the human prostate with the seminal vesicle: morphology, immunohistochemistry, and cell kinetics*, Prostate, 2005, 62(3):260–266.
- [16] Cunha GR, Hayward SW, Dahiya R, Foster BE, *Smooth muscle–epithelial interactions in normal and neoplastic prostatic development*, Acta Anat (Basel), 1996, 155(1):63–72.
- [17] Niu YN, Xia SJ, *Stroma–epithelium crosstalk in prostate cancer*, Asian J Androl, 2009, 11(1):28–35.
- [18] Cunha GR, Alarid ET, Turner T, Donjacour AA, Boutin EL, Foster BA, *Normal and abnormal development of the male urogenital tract. Role of androgens, mesenchymal–epithelial interactions, and growth factors*, J Androl, 1992, 13(6):465–475.
- [19] Schamhart DH, Kurth KH, *Role of proteoglycans in cell adhesion of prostate cancer cells: from review to experiment*, Urol Res, 1997, 25(Suppl 2):S89–S96.
- [20] Grossfeld GD, Hayward SW, Tlsty TD, Cunha GR, *The role of stroma in prostatic carcinogenesis*, Endocr Relat Cancer, 1998, 5(4):253–270.
- [21] Condon MS, *The role of the stromal microenvironment in prostate cancer*, Semin Cancer Biol, 2005, 15(2):132–137.

- [22] Tuxhorn JA, Ayala GE, Rowley DR, *Reactive stroma in prostate cancer progression*, J Urol, 2001, 166(6):2472–2483.
- [23] De Wever O, Mareel M, *Role of tissue stroma in cancer cell invasion*, J Pathol, 2003, 200(4):429–447.
- [24] Zhang Y, Nojima S, Nakayama H, Jin Y, Enza H, *Characteristics of normal stromal components and their correlation with cancer occurrence in human prostate*, Oncol Rep, 2003, 10(1):207–211.

**Corresponding author**

Iancu Emil Pleșea, Professor, MD, PhD, Department of Pathology, University of Medicine and Pharmacy of Craiova, 2–4 Petru Rareș Street, 200349 Craiova, Romania; Phone +40251–306 109, e-mail: pie1956@yahoo.com

*Received: September 15<sup>th</sup>, 2012*

*Accepted: December 18<sup>th</sup>, 2012*